

# Adaptive channels for data analysis and importance sampling

André van Hameren

*Institute of Nuclear Physics, NCSR Demokritos, Athens, Greece*

andrevh@inp.demokritos.gr

November 28, 2018

## Abstract

The adaptive multi-channel method is applied to derive probability distributions from data samples. Moreover, an explicit algorithm is introduced, for which both the channel weights and the channels themselves are adaptive, and which can be used both for data analysis and for importance sampling in Monte Carlo integration. Finally, it is pointed out how the usefulness for data analysis can be used to optimize the integration procedure.

PACS: 02.60.Pn; 02.70.Lq.

keywords: adaptive Monte Carlo integration; data analysis.

## 1 Introduction

Since its introduction in [1], adaptive multi-channeling has been extensively used as a help for importance sampling in numerical integration. The probability density, following which the integration points are generated, is written as a sum of densities with positive weights, and these weights are optimized during the integration process, in order to minimize the variance. The densities in the sum are called *channels*. In this paper, two variations of this method are introduced.

Firstly, we observe the similarity between the optimization of the density following which the integration points are generated, and the creation of a histogram in data-analysis. A histogram is a weighted sum of densities, given by the normalized non-overlapping indicator functions of subsets of the space in which the data-points take their values. These indicator functions are the ‘bins’. The optimal weights are estimated by the number of data points in the bins, and these are exactly the maximum likelihood estimators. In this paper, we will see that a histogram is a special case of the result of the application of a multi-channel method to derive the probability distribution. This will lead to ‘generalized histograms’ or *unitary probability decompositions* (u.p.d.s), by the use of general probability densities instead of the indicator functions. In Section 2, it will be pointed out how the weights can be optimized.

Secondly, we note that the adaptation in the application of the multi-channel method to importance sampling has mainly been applied to the *weights* in the sum of weighted densities. The channels themselves are fixed, which presupposes some knowledge about the integrand based upon which the particular channels have been chosen. If one does not want to rely on such knowledge to much, one can try to adapt also the channels. The simplest way to do this is by discarding channels with low weight during the integration process, or choosing new sets of channels from a larger given pool of channels [2]. A more advanced way of channel adaptation would be in the spirit of the VEGAS-algorithm [3] or the FOAM-algorithm [4], by creating new channels based on statistical analyses of the existing channels. The disadvantage of the first algorithm is that it is of limited efficiency in more than one dimension if the integrand has non-factorizable peak structures. The disadvantage of the second algorithm is that its complexity increases factorially with the dimension of the integration space. The problem with VEGAS can be solved if some information about the integrand is available, through the use of various channels corresponding with different coordinate systems [5].

In Section 3, the algorithm PARNI will be introduced. It uses adaptive multi-channeling, with channels that are fully adaptive themselves. It has no *a priori* problems with non-factorizable peak structures in the integrand, and its complexity grows linearly with the dimension of the integration space. Except for automatic importance sampling in Monte Carlo integration, PARNI can also be used for the creation of a u.p.d.. In Section 4 we will see how this property can be used to optimize the integration process, and this strategy will be applied to a problem in phase space integration.

## 2 Multi-channeling for data analysis

The derivation of a probability distribution from a sample of data is a common problem in scientific research. The idea is that such a distribution exists *a priori*, and that the data are drawn at random. The Bayesian interpretation then tells us that the *a priori* distribution (a.p.d.) gives the probability for this particular sample of data to be drawn. The frequentist interpretation tells us that estimators, calculated with the sample, will converge to the same values as the ones from the a.p.d. if the sample becomes very large. This interpretation can be translated into the statement that the distribution of the sample converges to the a.p.d. if the sample becomes large.

An obvious way to derive this distribution is by using such estimators, and the assumption that the distribution belongs to a class that can be completely described by the parameters that are estimated. In most cases, the original problem is even stated such, that the distribution is of a class that can be completely described by a set of parameters, and that one only wants to determine the correct values of these parameters. Part of the problem then becomes the determination of the right estimators, for example the maximum likelihood.

One particular kind of estimators are the number of data points in subsets of the space in which the data points take their values. Such a number, divided by the total number of data points, estimates the integral of the a.p.d. over the subset. The estimates for a collection of non-

overlapping subsets, or *bins*, that cover the whole space constitute a *histogram*, and in certain limits in which the number of bins and the number of data go to infinity, one can speak about convergence of the histogram to the probability density of the a.p.d..

A histogram is a weighted sum of densities, given by the normalized indicator functions of the subsets. The estimators described above are exactly the maximum likelihood estimators of these weights. In this section, we will see that a histogram is a special case of the result of the application of the multi-channel method to derive the probability distribution, and we will see how to generalize it to a *unitary probability decomposition* (u.p.d.), by the use of general probability densities instead of the indicator functions.

## 2.1 Maximum likelihood and entropy

If data points are assumed to be distributed following a probability density which is given up to the values of certain parameters, the maximum likelihood gives estimators for these parameters. For our application, it will be more convenient to formulate the maximum likelihood method in terms of the maximization of an entropy. The space in which data points  $\omega$  take their values is denoted  $\Omega$ , and this space may be multi-dimensional. The entropy of a probability density  $P$  on  $\Omega$  is given by

$$H(P) = \int_{\Omega} P(\omega) \log P(\omega) d\omega .$$

It can be used to determine the probability distributions of a system for which some information is available. This information could be the values of characteristics like mean and variance, but could also be knowledge that  $P = G_x$ , where  $G_x$  is given up to the values of the parameters  $x = (x_1, x_2, \dots, x_n)$ . The shape of  $P$ , or the values of  $x$ , should be such that the entropy assumes its maximum value <sup>1</sup>.

But we are interested in a different situation, with a sample or a stream of data as the only information available. So the *a priori* probability density  $P$  is given somehow, and we do not know it, but want to approximate it with the help of the data, using a parametrized density  $G_x$ , specially chosen for this task.  $P$  defines a probability measure on  $\Omega$ , and for a measurable function  $f$  we write

$$\langle f \rangle_P := \int_{\Omega} f(\omega) P(\omega) d\omega .$$

In search for the optimal values of  $x$ , we introduce the entropy of  $G_x$  relative to  $P$ :

$$H(P; G_x) := \langle \log G_x \rangle_P . \tag{1}$$

It is the original entropy with  $\log P$  replaced by  $\log G_x$ , and naturally, one would expect that if  $x$  is optimal, then the two entropies are close together. Encouraged by this expectation, we state that

**Principle 1**  $x$  is optimal if  $H(P; G_x)$  assumes its maximum value.

---

<sup>1</sup>Or such that  $-H(P)$  assumes its minimal value.

Extrema of  $H(P; G_x)$  are given by solutions of the equations

$$0 = \frac{\partial}{\partial x_i} H(P; G_x) = \frac{\partial}{\partial x_i} \langle \log G_x \rangle_P, \quad i = 1, \dots, n .$$

The connection with the maximum likelihood can be established by realizing that, in real life, one does not know  $P$ , so that integrals over  $\Omega$  have to be estimated with the help of the available data, which are distributed following  $P$ . In fact, if  $\omega = (\omega_1, \omega_2, \dots, \omega_N)$  is such a sample of data points, and if  $\langle f^2 \rangle_P$  exists, then

$$\langle f \rangle_\omega := \frac{1}{N} \sum_{k=1}^N f(\omega_k) \xrightarrow{N \rightarrow \infty} \langle f \rangle_P ,$$

where convergence takes place at least in probability, like in Monte Carlo integration. Using this estimator for the integral, the equations become

$$0 = N \frac{\partial}{\partial x_i} \langle \log G_x \rangle_\omega = \frac{\partial}{\partial x_i} \sum_{k=1}^N \log G_x(\omega_k) = \frac{\partial}{\partial x_i} \log \prod_{k=1}^N G_x(\omega_k) ,$$

so that solutions give extrema of the likelihood function. We prefer to stick to the entropy formulation from now on, because it seems more appropriate in the case of a continuous data stream, a situation that resembles the one of Monte Carlo integration, where a continuous stream of data points is generated in order to integrate a function.

## 2.2 Entropy and multi-channeling

From now on,  $G_x$  will always be linear in the parameters  $x = (x_1, x_2, \dots, x_n)$ , and be defined with the help of  $n$  probability densities  $g_i$ , or *channels*, by

$$G_x(\omega) = \sum_{i=1}^n x_i g_i(\omega) . \quad (2)$$

The parameters, or *weights* will always be positive, and normalized such that  $\sum_{i=1}^n x_i = 1$ . If we look for extrema of the entropy (1), we have to take care that the weights stay normalized, and instead of including this normalization in  $G_x$  explicitly, we prefer to extend the entropy with the help of a Lagrange multiplier. So we want to find the maximum of

$$H(P; G_x, \lambda) := \langle \log G_x \rangle_P - \lambda \left( 1 - \sum_{i=1}^n x_i \right)$$

with respect to  $x$  and  $\lambda$ . Extrema are solutions to the equations

$$\langle g_i / G_x \rangle_P = \lambda, \quad i = 1, \dots, n \quad \text{and} \quad \sum_{i=1}^n x_i = 1 .$$

The value of the Lagrange multiplier  $\lambda$  can be found by multiplying the equation  $\langle g_i/G_x \rangle_P = \lambda$  with  $x_i$  and taking the sum over  $i$ . Remembering (2), we then find that  $\lambda = 1$ .

The question is now whether this solution corresponds to a maximum, and performing an analysis like in [1], we can establish that it leads to at least a local maximum: denoting the solution by  $\bar{x}$  and taking a small variation  $\varepsilon = (\varepsilon_1, \dots, \varepsilon_n)$  with  $\sum_{i=1}^n \varepsilon_i = 0$ , around the solution we find

$$H(P; G_{\bar{x}+\varepsilon}, 1) = H(P; G_{\bar{x}}, 1) - \frac{1}{2} \langle G_{\varepsilon}^2/G_{\bar{x}}^2 \rangle_P + \mathcal{O}(\varepsilon^3) ,$$

and we see that small variations lead to a decrease of the entropy. We can re-formulate Principle 1 now, and state that if  $G_x$  is a weighted sum of channels  $g_i$ , then

**Principle 2**  $x$  is optimal if the  $\langle g_i/G_x \rangle_P$  are equal (to 1) for all  $i = 1, \dots, n$ .

### 2.3 Numerical path to the solution

In general it is difficult to find an analytic solution to the problem posed by Principle 2. We can, however, try to find the solution, or at least an approximation, by numerical methods. We follow the same path as in [1] (Appendix A), by considering the case in which the channels  $g_i$  are normalized indicator functions of non-overlapping subsets of  $\Omega$  with volume  $v_i$ , so that  $G_x$  is a histogram. Let  $\vartheta_i = v_i g_i$  denote the indicator functions. Then

$$\langle g_i/G_x \rangle_P = \frac{1}{x_i} \langle \vartheta_i \rangle_P \quad \text{so that the solution is given by } x_i = \langle \vartheta_i \rangle_P .$$

So the optimal weight of channel  $g_i$  is given by to the integral of the probability density over the subset corresponding to the indicator function. The weight for the indicator function is then given by  $x_i/v_i$ : the height of the bin, like usually for a histogram. We observe now that, starting from any  $x$ , the successive operations

**Algorithm 1 (unitary probability decomposition)**

1.  $y_i \leftarrow x_i \langle g_i/G_x \rangle_P$  for all  $i = 1, \dots, n$
2.  $x_i \leftarrow \frac{y_i}{\sum_{j=1}^n y_j}$  for all  $i = 1, \dots, n$

lead directly to the optimal values for  $x$ , and this gives us faith to seek for the solution in the general case by recursive application of these operations.

In real life again, we cannot calculate  $\langle g_i/G_x \rangle_P$ , and have to estimate it with an available sample  $\omega$  by  $\langle g_i/G_x \rangle_{\omega}$ . Notice that, in the case that  $G_x$  is a histogram,  $x_i \langle g_i/G_x \rangle_{\omega} = \langle \vartheta_i \rangle_{\omega}$  is the number of data points in bin  $i$ .

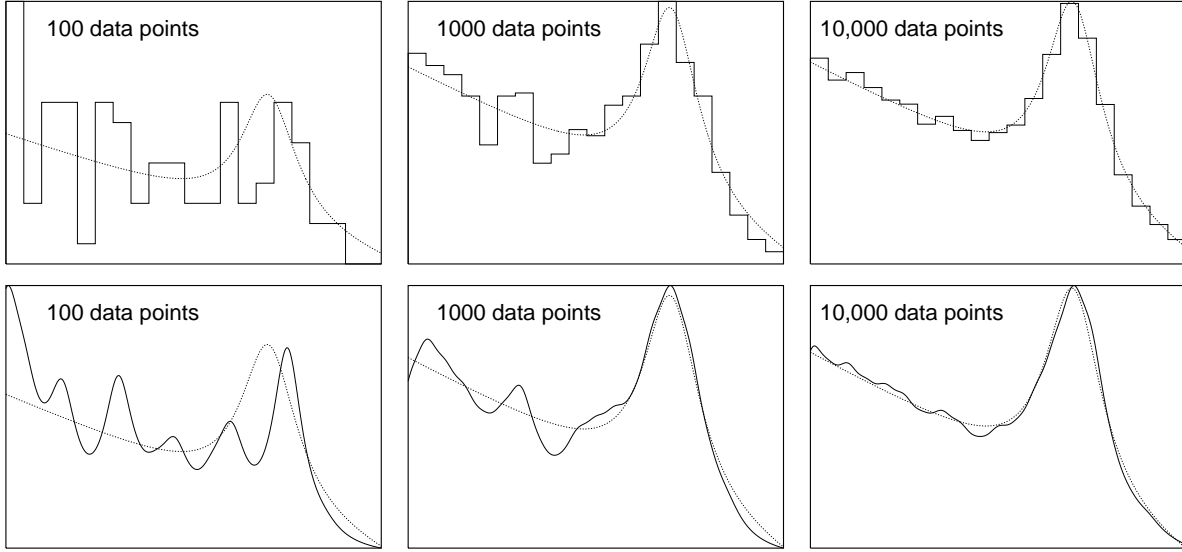


Figure 1: Histograms (upper graphs) and Cauchy-u.p.d.s (lower graphs) for random data-points, distributed following the dashed curve.

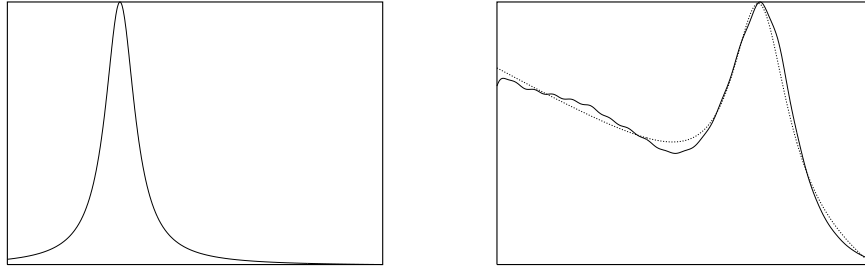


Figure 2: Left:  $g_7$  for  $n = 21$ . Right:  $10^4$  data points taken in batches of less than  $10^3$ , with only one iteration of Algorithm 1 for each batch.

## 2.4 An example of unitary probability decompositions

As a small application, we show how the above may be used to construct u.p.d.s. For simplicity, we consider the one-dimensional case of a histogram on the interval  $[0, 1]$ . Instead of  $n$  normalized indicator functions  $g_i(\omega) = n\theta(\omega - \frac{i-1}{n})\theta(\frac{i}{n} - \omega)$  of  $n$  bins with width  $1/n$ , we use  $n$  Cauchy densities

$$g_i(\omega) := \frac{A_i}{1 + \left(\frac{\omega - \omega_i}{\sigma_i}\right)^2} \quad \text{with} \quad \sigma_i = \frac{1}{n}, \quad \omega_i = \frac{i-1}{n-1},$$

and normalization  $1/A_i = \arctan\left(\frac{1-\omega_i}{\sigma_i}\right) + \arctan\left(\frac{\omega_i}{\sigma_i}\right)$ . The left of Figure 2 depicts  $g_7$  for  $n = 21$ . In Figure 1 we present the histograms (upper graphs) and Cauchy-u.p.d.s (lower graphs) for  $10^2$ ,  $10^3$  and  $10^4$  random data-points, distributed following the density depicted with the dashed curve in all graphs. Both types consist of 21 channels, and for the generalized type the value of the weights after a maximum of  $10^3$  iterations of Algorithm 1 is used.

For high number of data points, a high number of iterations becomes inappropriate, and in case of a data stream, the number of data points increases continuously. In those cases, batches of data points can be used, and Algorithm 1 can be applied once with each batch. In order to choose a size for the batches, we take into account the common rule that, in a normal histogram, every bin should contain at least a few data points in order to trust it. The number of data points from a sample  $\omega = (\omega_1, \omega_2, \dots, \omega_N)$  in the bin corresponding to indicator function  $\vartheta_i = v_i g_i$  is given by

$$\sum_{k=1}^N \vartheta_i(\omega_k) = N v_i \langle g_i \rangle_{\omega} = N \frac{\langle g_i \rangle_{\omega}}{\langle g_i^2/P \rangle_P},$$

and we can use this for the general case. Of course,  $\langle g_i^2/P \rangle_P$  can only be estimated, for example with  $\langle g_i^2/G_x \rangle_{\omega}$ . The right of Figure 2 shows the result with  $10^4$  random data points, taken in batches. The size of the batches was such that the ‘generalized number of data points’ for each channel was at least 35, which happened to lead to batches with not more than  $10^3$  data points.

### 3 Multi-channeling with adaptive channels

In the discussion so far, the channels  $g_i$  were fixed, and the only adaptation appeared for the weights  $\chi_i$ . As described in the introduction, it would be attractive to also adapt the channels. We introduce the algorithm PARNI<sup>2</sup> in which this is achieved. We consider the  $s$ -dimensional hypercube  $\Omega = [0, 1]^s$ . The channels are all normalized indicator functions, which are, however, not necessarily non-overlapping. The subsets corresponding to the indicator functions will only be *boxes* of the type  $[a_1, b_1] \times [a_2, b_2] \times \dots \times [a_s, b_s]$ .

#### Algorithm 2 (PARNI)

1. We start with  $2s$  channels corresponding to all pairs of boxes obtained by dissecting  $\Omega$  in two along the Cartesian directions.

In the case of the data stream, data points are generated from an external source, and in the case of numerical integration, they are generated from  $G_x$ , the density constructed with the channels and the weights. For completeness, we repeat the algorithm to generate the points in the case of numerical integration:

2. choose a channel with a probability equal to the weight of the channel;
3. generate a point in the box corresponding to the channel, uniformly distributed.

A batch of data is collected, and

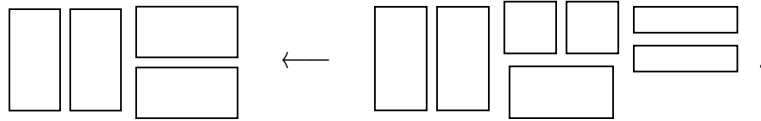
4. depending on the task, Algorithm 1 or Algorithm 3 (Appendix A) is applied to optimize the weights.

---

<sup>2</sup>Practical Adaptive Random Number Idealizer.

5. Directly after an optimization step, the box with the highest weight is replaced by 2s boxes, obtained in pairs by dissecting the original box in two along the Cartesian directions.

This step makes the algorithm fully self-adaptive. Executed for the first time in two dimensions, this step could look as follows



The 4 overlapping boxes on the l.h.s. cover the integration space twice. We just drew them in pairs next to each other for clarity. Suppose the upper right box has the largest weight. Then it is replaced<sup>3</sup> by the smaller boxes on the r.h.s., so that we end up with 7 overlapping boxes which cover the integration space  $2\frac{1}{2}$  times. The addition of boxes cannot be continued forever in practice, and one would like to restrain the number of channels to a maximum.

6. If the number of channels reached its maximum, boxes with the smallest weights can be merged by replacing them by the smallest possible (new) box that contains all of them.

Notice that this last procedure is very simple for Cartesian boxes. Also notice that the merging of boxes is necessary, and that one should not just throw away boxes, because of the danger of ending up with ‘holes’ in the integration space. Of course, the last two steps can be repeated a few times before gathering new data points in order to replace more channels at once and possibly accelerate the optimization process.

One could ask the question why using all the overlapping boxes, and not use just one new pair in each step. The answer to this question is simply stated by a new question: which pair? The idea is to let the algorithm for the weight optimization decide which new boxes are going to be important. Of course, the number of new overlapping boxes in each step grows with the dimension of the integration space, but not drastically, only linearly.

Another question could be why to use boxes in the first place, and why not some other geometrical objects. The answer to this question is, firstly, the fact that the complexity of the algorithm runs the risk of exploding with the dimension of  $\Omega$ . For example, the minimal number of  $s$ -simplices needed to fill  $[0, 1]^s$  is  $s!$ , while the number of boxes needed is 2. Secondly, there is the practical simplicity to encode the boxes.

### 3.1 A simple application in two dimensions

We present some results with probability density, or integrand,

$$P(\omega) \propto \frac{1}{(0.02)^2 + (\omega_1 + \omega_2 - 1)^2} , \quad (3)$$

where the normalization is not written down explicitly for convenience. The choice for this

<sup>3</sup>Replacements or assignments are denoted with the arrow pointing to the left:  $a \leftarrow b$  means ‘ $b$  is put in the memory space of  $a$ ’.



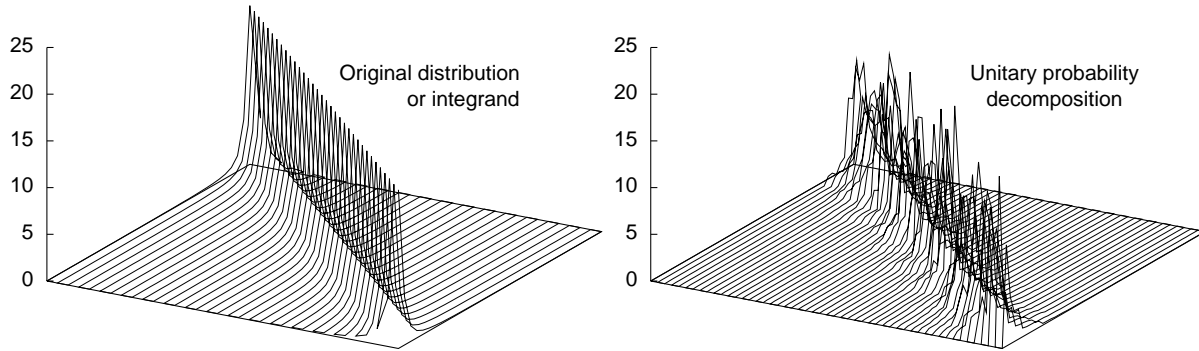


Figure 3: Left:  $P(\omega)$  from (3). Right: Unitary probability decomposition  $G_x$  after  $10^5$  data points distributed following  $P$ .

method	all $10^5$ data points			last $10^3$ data points		
	result	error	eff.	result	error	eff.
integration with variance optimization	0.9977	0.0031	0.0156	1.004	0.014	0.259
integration after u.p.d. creation	0.9980	0.0016	0.0865	0.996	0.016	0.167
integration without optimization	1.0015	0.0089	0.0588	1.093	0.093	0.059

Results for the integration of density (3).

particular density is taken from [4]. It is interesting because it is not factorizable, and VEGAS performs badly when used to integrate it. Since PARNI uses the Cartesian boxes, also here this density constitutes a serious test. All results with PARNI were obtained with a maximal number of 1000 channels, batches of 1000 data points for the multi-channel optimization, and with 20 iterations of steps 5 and 6.

The results for the integration of (3) are collected in Figure 3. Given are the result (average weight), the estimated error (standard deviation) and the efficiency (average weight divided by maximum weight).

For the method ‘integration with variance optimization’, we see the effect of the optimization if we compare the result of the last  $10^3$  data points with the result using all data points: the efficiency improves and the estimated error is less than 10 times worse, the ‘10’ being expected from the  $1/\sqrt{N}$ -rule of Monte Carlo integration.

For the method ‘integration after u.p.d. creation’, first  $10^5$  data points distributed following (3) were generated to create the u.p.d., and then  $10^5$  integration points were generated using this u.p.d. to integrate (3). So observing that the result is better than in the case of variance optimization, one should keep in mind that twice as many data points have been used. Furthermore, this method of integration cannot be considered useful as long as we do not specify how to generate the first  $10^5$  data points. We will address this issue in Section 4. For now, the “smallness” of the error estimate should be interpreted as a measure of the “goodness” of the u.p.d..

The results of integration without any optimization are also included for comparison. Notice

that in that case, the efficiency including the total amount of data is actually better than in the case of variance optimization. Apparently, the optimization process for PARNI needs some trail-and-error in the beginning to end up at the results for the last 1000 data points, which are obviously better than for the non-optimized case. This problem becomes more apparent in more-dimensional applications and can be solved following the method of ‘integration after u.p.d. creation’, as we will see in Section 4.

### 3.2 Application to phase space integration

In the following, some results from the application of PARNI in phase space integration are presented. We consider the problem of calculating

$$\int d\Phi_n(Q; m_1^2, \dots, m_n^2; p_1, \dots, p_n) A(p_0, p_1, \dots, p_n, p_{n+1}) , \quad (4)$$

with

$$d\Phi_n(Q; m_1^2, \dots, m_n^2; p_1, \dots, p_n) = \left( \prod_{i=1}^n d^4 p_i \delta(p_i^2 - m_i^2) \theta(p_i^0) \right) \delta\left(Q - \sum_{i=1}^n p_i\right) , \quad (5)$$

and integrand

$$A(p_0, p_1, \dots, p_n, p_{n+1}) = \frac{(2\pi)^{4-3n} \prod_{j>i=0}^{n+1} \theta((p_i \cdot p_j) - s_c)}{(p_0 \cdot p_1)(p_1 \cdot p_2)(p_2 \cdot p_3) \cdots (p_n \cdot p_{n+1})(p_{n+1} \cdot p_0)} , \quad (6)$$

where  $(p_i \cdot p_j)$  denotes the Lorentz invariant scalar product,  $p_0 = (\frac{1}{2}, 0, 0, \frac{1}{2})$  and  $p_{n+1} = (\frac{1}{2}, 0, 0, -\frac{1}{2})$ . The problem in calculating this integral is the pole structure in the scalar products of the integrand. Although the integrand is regularized by a cut-off  $s_c$  in these scalar products, it still has a peak structure that makes convergence in a straightforward numerical calculation problematic. Integrals with this type of singularity structures are typically found in the phase space integration of QCD amplitudes, and they are called *antenna pole structures* [2, 6].

The straightforward numerical (Monte Carlo) calculation would consist of the generation of  $n$  random momenta  $p_i$  uniformly distributed in phase space, the bounded  $(3n - 4)$ -dimensional subspace of  $\mathbf{R}^{4n}$  encoded in  $d\Phi$ , and the calculation of the average of the integrand. Each set of random momenta is constructed from a set of random numbers between 0 and 1, and the idea is now to let PARNI deliver these numbers. For the construction of the momenta, there are two algorithms on the market: RAMBO, which uses the so-called *democratic* approach [7], and the hierarchical construction of momenta (HICOM). The disadvantage of RAMBO for our application is that it needs  $3n$  instead of  $3n - 4$  random numbers per  $n$  momenta, and we want to keep the dimension as low as possible<sup>4</sup>. Furthermore, the freedom one has in the actual implementation of HICOM allows for an algorithm that is completely equivalent with RAMBO in the case of massless momenta. This implementation is presented in Appendix B.

---

<sup>4</sup>The original code by R. Kleiss uses  $4n$  random numbers per  $n$  momenta, but this can easily be reduced to  $3n$  with little extra cost.

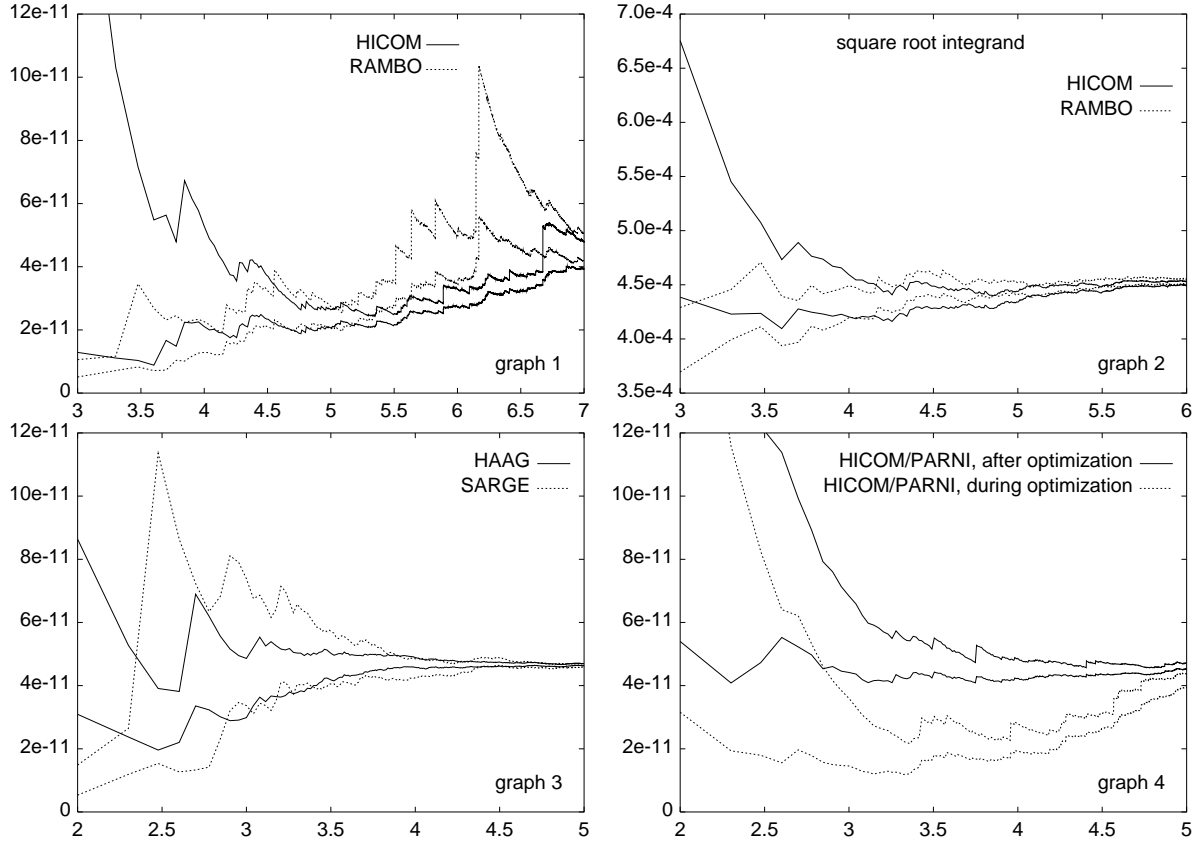


Figure 4: The process of convergence during the Monte Carlo calculation of (4) for  $n = 4$  massless momenta with center of mass energy  $\sqrt{Q^2} = 1000 \text{ GeV}$  and  $s_c = 450 \text{ GeV}^2$ . Along the horizontal axis runs  $^{10}\log(\#\text{ events})$ . Two curves of the same type give the average *plus* the standard deviation and the average *minus* the standard deviation.

Figure 4 shows the results for the case of  $n = 4$  massless momenta with a center of mass energy  $\sqrt{Q^2} = 1000 \text{ GeV}$  and a cut-off  $s_c = 450 \text{ GeV}^2$ . There, the process of convergence during the Monte Carlo integration is shown. Along the horizontal axis runs  $^{10} \log N$ , where  $N$  is the number of generated events (sets of momenta). In each graph, the two curves of the same type give the average *plus* the standard deviation and the average *minus* the standard deviation after the number of events on the horizontal axis.

Graph 3 shows the result with phase space generators HAAG and SARGE, which were specially designed to integrate functions with antenna pole structures [2, 6]. This is how a decent Monte Carlo integration process should look like. The standard deviations converge to zero and the average moves around a straight line: the process is unbiased and the estimated error can be trusted at any point.

SARGE and HAAG were developed to cure graph 1, the result with HICOM and RAMBO. The standard deviations hardly converge and the estimated error cannot be trusted at all: as long as no event hits a peak, the average is an under estimation. If an event hits a peak, the standard deviation increases drastically. Notice that the horizontal axis runs over 100 times more events than in graph 3. Because of the particular peculiar behavior of HICOM in this run, graph 2 with the result of the integration of the square root of the integrand, which has a much softer singular behavior, is included. We see a decent Monte Carlo process again and see that HICOM behaves the same as RAMBO.

Graph 4, finally, depicts the results with HICOM in combination with PARNI. For the curve ‘during optimization’, PARNI started from scratch. We see the peculiar behavior of HICOM back in this run, for which PARNI tries to compensate. PARNI used a maximal number of 1000 channels, batches of 1000 data points for the multi-channel optimization with Algorithm 3, and 4 iterations of steps 5 and 6. After the generation of  $10^5$  events, the channels of PARNI were stored, and the process was repeated starting with these channels, leading to the curves ‘after optimization’, which show a decent Monte Carlo process again.

## 4 The use of u.p.d.s in numerical integration

The behavior of PARNI during optimization in Figure 4 is what one would naturally expect from a general-purpose self adaptive Monte Carlo integration systems. A general-purpose system starts with no information about the integrand, and cannot do anything else then start with generating integration points distributed uniformly over the integration space. If the integrand has sharp peaks, there is no enhanced probability for the system to hit these peaks in the beginning, and an under estimation of the integral is the result. One can imagine the extreme case of an integrand consisting of a sum of delta-peaks, for which the probability to see them is zero.

A solution to this problem is given by the possibility to create a u.p.d. before starting with the integration. This u.p.d. can then serve as a starting point for the self adaptive integration system. In order to create the u.p.d., one needs a stream of data points that are distributed following a density that looks like the integrand. This stream of data will immediately show the peak

structure, and in the extreme case mentioned before it will *only* show the delta-peaks. Important in this idea is that we realize that the creation of such a stream is, in principle, an easier problem than the integration problem: one can, for example, use the Metropolis algorithm.

Since we want to restrict ourselves to integration problems in phase space like in the previous section, we refer to [8] for the use of the Metropolis algorithm. The disadvantage of this algorithm for the use of integration is that, although it creates a stream of data points that are distributed following any normalized positive function on the integration space, it does not give this normalization, the determination of which usually is the actual integration problem one wants to solve.

In the application we just described this normalization is not needed. Having in mind, however, that the evaluation of the integrand is expensive, we want to use all these evaluated integration points as efficiently as possible. Let us denote

$$\langle f \rangle_P := \frac{\int_{\Omega} f(\omega) P(\omega) d\omega}{\langle P \rangle} \quad , \quad \langle P \rangle := \int_{\Omega} P(\omega) d\omega$$

for any integrable positive bounded function  $P$  on the integration space  $\Omega$ . With the Metropolis algorithm, one can estimate  $\langle f \rangle_P$  for any quadratically integrable  $f$ , but one cannot calculate  $\langle P \rangle$ . Inspired by the solution to this problem proposed in [8], we observe that

$$\langle P \rangle = \langle P^{1-\alpha} \rangle_{P^\alpha} \langle P^\alpha \rangle$$

for any  $\alpha \in [0, 1]$ . We also observe that the function  $P^\alpha$  will be easier to integrate than  $P$  itself because the peaks are suppressed. There is an equilibrium: for small  $\alpha$  the calculation of  $\langle P^\alpha \rangle$  will be easy, but the estimation of  $\langle P^{1-\alpha} \rangle_{P^\alpha}$  will be difficult, whereas for  $\alpha$  close to 1 the estimation of  $\langle P^{1-\alpha} \rangle_{P^\alpha}$  will be easy, but the estimation of  $\langle P^\alpha \rangle$  difficult. Important in light of the foregoing is that *the estimation of  $\langle P^{1-\alpha} \rangle_{P^\alpha}$  will serve a stream of data points distributed following  $P^\alpha$  which can be used to create a u.p.d. for the estimation of  $\langle P^\alpha \rangle$* . This sounds tricky, like one uses integration points twice, but this is not the case. The integration points used to estimate  $\langle P^{1-\alpha} \rangle_{P^\alpha}$  are used to initialize an integration system to calculate  $\langle P^\alpha \rangle$  with new integration points.

The question that remains is what value to choose for  $\alpha$ . We shall stick to values close to 1, so that the estimation of  $\langle P^{1-\alpha} \rangle_{P^\alpha}$  is relatively easy, and the problem of calculating  $\langle P^\alpha \rangle$  is close to the original integration problem.

## 4.1 Application to phase space integration

It appears that PARNI performs better with a small change in the algorithm, namely by merging a number of boxes after every optimization step, so by performing step 6 even before the maximum allowed number of channels has been reached. The positive effect must be a result of the gain in flexibility. For the following calculations, a maximum number of 4000 channels has been used, with an optimization step after every 4000 events. During every such step, more-or-less 50 boxes were merged and step 5 was iterated as many times as it takes to add more-or-less 120 boxes.

Another advantage of the use of HICOM instead of RAMBO in combination with PARNI shows up for the use of the hybrid Metropolis procedure sketched before, namely the fact that the mapping from random points in the  $(3n-4)$ -dimensional hypercube to momenta is invertible. This means that, for the initialization of PARNI through the creation of the u.p.d., the momenta generated with the Metropolis algorithm as described in [8] can be used. One could, of course, use another implementation of the Metropolis algorithm in the  $(3n-4)$ -dimensional hypercube and map these points to momenta, but we do not want to go into this issue at this stage, not in the least place because of the (extreme) simplicity of the algorithm from [8].

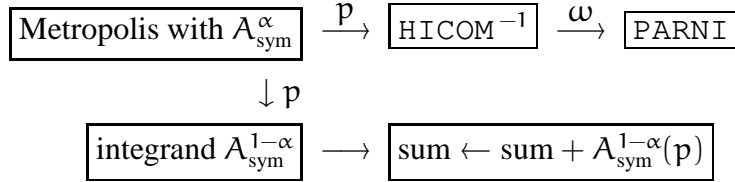
We apply all this to the problem of calculating (4), with the function  $A$  replaced by a sum over permutations of its arguments, so that the integrand looks more like a QCD-amplitude: so we want to calculate

$$\langle A_{\text{sym}} \rangle := \int d\Phi_n(Q; m_1^2, \dots, m_n^2; p_1, \dots, p_n) A_{\text{sym}}(p_0, p_1, \dots, p_n, p_{n+1}) , \quad (7)$$

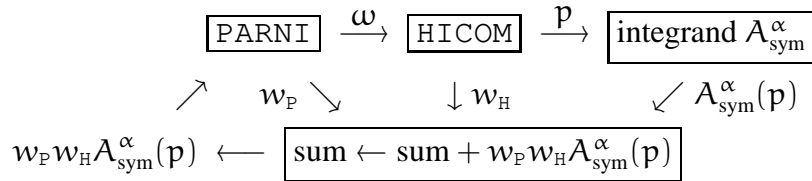
with

$$A_{\text{sym}}(p_0, p_1, \dots, p_n, p_{n+1}) = \sum_{\pi \in \text{Sym}(n+1)} A(p_0, p_{\pi(1)}, \dots, p_{\pi(n)}, p_{\pi(n+1)}) ,$$

and with  $d\Phi_n$ ,  $A$  as in (5), (6). Below we put the integration process for the calculation of  $\langle A_{\text{sym}}^{1-\alpha} \rangle_{A_{\text{sym}}^\alpha}$  and the initialization process of PARNI in a flow chart. The variables are the set  $p$  of  $n$  momenta and  $\omega \in [0, 1]^{3n-4}$ .



In the chart for the integration process of  $\langle A_{\text{sym}}^\alpha \rangle$  and further optimization of PARNI, also the weight factors coming from PARNI and HICOM are included:



The results are presented in Figure 5 for  $n = 4$ , and in Figure 6 for  $n = 6$ . The parameter  $\alpha$  was put to 0.9 for all cases.

We start the discussion with the results for  $n = 4$ . In order to obtain the curves with the title ‘Metropolis’ in graph 1, the calculation of  $\langle A_{\text{sym}}^\alpha \rangle$  was done first with SARGE, so that  $\langle A_{\text{sym}} \rangle = \langle \langle A_{\text{sym}}^\alpha \rangle A_{\text{sym}}^{1-\alpha} \rangle_{A_{\text{sym}}^\alpha}$  could be calculated directly with the metropolis algorithm. In a realistic calculation this is not necessary: this has only been done in order to arrive at curves at the same scale as the curves from HAAG and graph 2. The Metropolis-curves converge rather quickly, as expected since the weights do not fluctuate much because of the suppression from the exponentiation with  $1 - \alpha$ .

Graph 2 depicts the process of convergence in the direct calculation of  $\langle A_{\text{sym}} \rangle$  with PARNI and RAMBO. The latter under estimates the integral for many events and hardly converges. PARNI starts converging quickly after  $10^5$  events, obviously after the optimization took place.

The fact that the estimated errors with RAMBO in graph 2 cannot be trusted becomes clear from the curves in graph 3 for the calculation of  $\langle A_{\text{sym}}^\alpha \rangle$ , which is supposed to be (slightly) easier for RAMBO, while the curves look worse. Graph 4 depicts the curves from PARNI for the calculation of  $\langle A_{\text{sym}}^\alpha \rangle$ , both with and without initialization using the data from the metropolis calculation of  $\langle A_{\text{sym}}^{1-\alpha} \rangle_{A_{\text{sym}}^\alpha}$ . And clearly the curves with initialization converge faster.

For  $n = 6$ , the graphs look more-or-less the same: the curves from RAMBO hardly converge or constitute an under estimation, while the curves from PARNI *do* converge. Furthermore, the curves with initialization reach a given estimated error sooner than without initialization.

The tables coming with the figures speak for themselves, except maybe of the last two columns. These give a measure of the computation time, “normalized” with respect to the reached error. The first of the last two columns gives this number for the actual calculation, in units of the computation time of the integrand. The last column gives this number extrapolated to the case that the evaluation of the integrand would be much more expensive than the generation of events. For RAMBO, which can be considered to be a very cheap algorithm, these numbers are close to each other<sup>5</sup>. The conclusion that can be drawn from the tables is that PARNI performs much better than RAMBO, and that PARNI performs better with initialization than without. The reason why HAAG and SARGE perform much better than the rest is that these algorithms have been specially designed to integrate exactly  $A_{\text{sym}}$ .

---

<sup>5</sup>The odd situation with Metropolis for  $n = 6$ , where the first number is smaller than the second, is a result of the fact that a data point is re-used if a new one is not accepted, and does not add to the computation time.

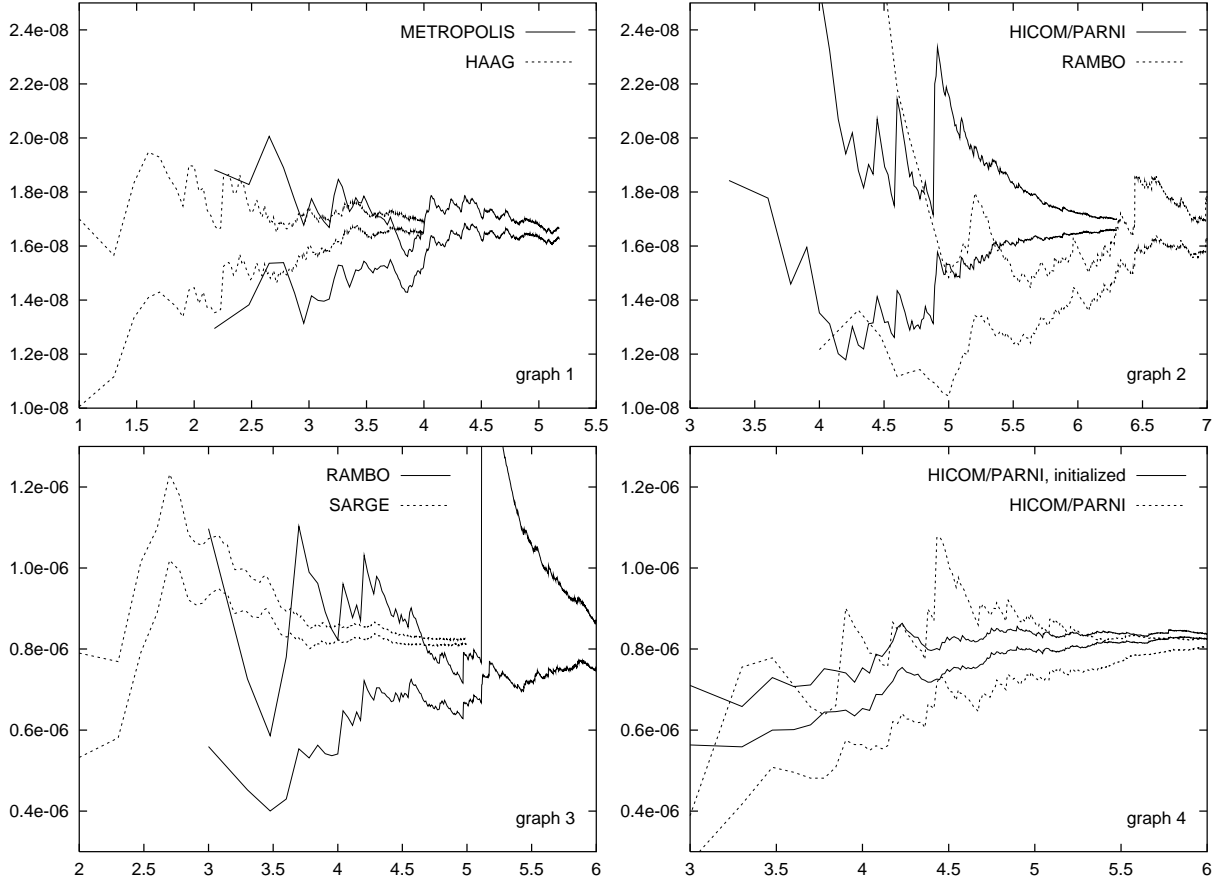


Figure 5: The process of convergence during the Monte Carlo calculation of (7) for  $n = 4$  massless momenta with center of mass energy  $\sqrt{Q^2} = 1000 \text{ GeV}$  and  $s_c = 450 \text{ GeV}^2$ . Along the horizontal axis runs  $^{10}\log(\# \text{ events})$ . Two curves of the same type give the average *plus* the standard deviation and the average *minus* the standard deviation.

integrand	graph	algorithm	I $10^{-8}$	$\sigma$ %	N $10^3$	$\sigma^2 T_{\text{tot}}/T_{\text{int}}$ $10^3$	$\sigma^2 N_{\text{acc}}$ $10^3$
$A_{\text{sym}}$	1	Metropolis	1.649	1.11	150	0.0458	0.0186
		HAAG	1.669	1.27	10	0.0261	0.00113
	2	PARNI	1.670	1.17	2000	3.03	0.211
		RAMBO	1.718	4.70	10000	22.7	20.9
$(A_{\text{sym}})^{0.9}$	3	SARGE	81.89	0.728	100	0.00828	0.00247
		RAMBO	81.17	7.11	1000	5.20	4.79
	4	PARNI, initialized	83.16	0.732	1000	0.587	0.043
		PARNI	81.66	1.21	1000	1.55	0.121

The final results corresponding with Figure 5. I is the integral,  $\sigma$  the standard deviation, N the number of generated events,  $T_{\text{tot}}$  the total computation time,  $T_{\text{int}}$  the time it takes to perform one evaluation of the integrand and  $N_{\text{acc}}$  the number of accepted (non-zero weight) events.



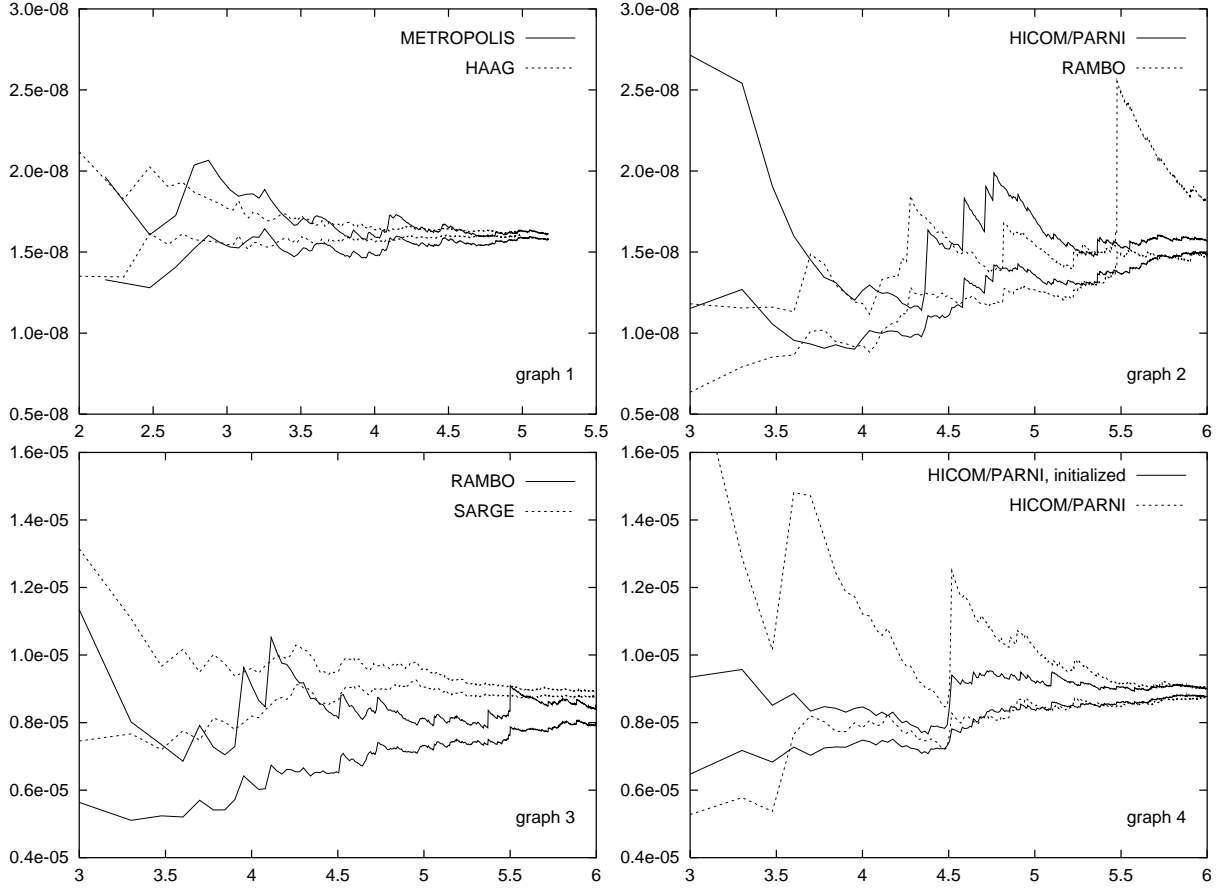


Figure 6: The process of convergence during the Monte Carlo calculation of (7) for  $n = 6$  massless momenta with center of mass energy  $\sqrt{Q^2} = 1000 \text{ GeV}$  and  $s_c = 450 \text{ GeV}^2$ . Along the horizontal axis runs  $^{10}\log(\# \text{ events})$ . Two curves of the same type give the average *plus* the standard deviation and the average *minus* the standard deviation.

integrand	graph	algorithm	I $10^{-8}$	$\sigma$ %	N $10^3$	$\sigma^2 T_{\text{tot}}/T_{\text{int}}$ $10^3$	$\sigma^2 N_{\text{acc}}$ $10^3$
$A_{\text{sym}}$	1	Metropolis	1.594	1.04	150	0.0134	0.0163
		HAAG	1.617	0.713	100	0.0122	0.00139
	2	PARNI	1.528	2.58	1000	0.664	0.468
		RAMBO	1.647	10.0	1000	8.03	7.44
$(A_{\text{sym}})^{0.9}$	3	SARGE	885.6	0.866	1000	0.00424	0.00264
		RAMBO	823.9	3.14	1000	0.765	0.732
	4	PARNI, initialized	889.4	1.32	1000	0.167	0.118
		PARNI	886.8	1.69	1000	0.273	0.198

The final results corresponding with Figure 6. I is the integral,  $\sigma$  the standard deviation, N the number of generated events,  $T_{\text{tot}}$  the total computation time,  $T_{\text{int}}$  the time it takes to perform one evaluation of the integrand and  $N_{\text{acc}}$  the number of accepted (non-zero weight) events.

## 5 Summary

A histogram has been shown to be a special case of the application of the *multi-channel* method to derive a probability distribution from a sample, or a stream, of data. The channels are the normalized bins of the histogram, and the channel weights are the volumes of the bins. An algorithm has been presented how to optimize the weights in the case of channels that consist of arbitrary probability densities, leading to a *unitary probability decomposition* (u.p.d.).

Furthermore, the algorithm PARNI has been presented, for which not only the channel weights, but also the channels themselves are adaptive. It can be used both for the creation of u.p.d.s and for automatic importance sampling in Monte Carlo integration. It handles data in an  $s$ -dimensional hypercube  $[0, 1]^s$  for arbitrary  $s$ . It has no *a priori* problems with non-factorizable peak structures in the integrand, and its complexity grows linearly with  $s$ .

Finally, it has been shown how the property of PARNI to create a u.p.d. can be used to optimize the Monte Carlo integration procedure, and this has been applied to a problem in phase space integration.

### Acknowledgment

This research has been supported by a Marie Curie Fellowship of the European Community program “Improving Human Research Potential and the Socio-economic Knowledge base” under contract number HPMD-CT-2001-00105.

## References

- [1] R. Kleiss and R. Pittau, *Weight optimization in multichannel Monte Carlo*, Comp. Phys. Comm. **83** (1994) 141-146 (hep-ph/9405257).
- [2] A. van Hameren and C.G. Papadopoulos, *A hierarchical phase space generator for QCD antenna structures*, Eur. Phys. J. **C25** (2002) 563-574 (hep-ph/0204055).
- [3] G.P. Lepage, *A new algorithm for adaptive multidimensional integration*, J. Comp. Phys. **27** (1978) 192.
- [4] S. Jadach, *FOAM: multi-dimensional general purpose Monte Carlo generator with self-adapting simplicial grid*, Comp. Phys. Comm. **130** (2000) 244-259 (physics/9910004).
- [5] T. Ohl, *VEGAS revisited: adaptive monte carlo integration beyond factorization*, Comp. Phys. Comm. **120** (1999) 13-19 (hep-ph/9806432).
- [6] A. van Hameren, R. Kleiss and P. Draggiotis, *SARGE: An Algorithm for generating QCD antennas*, Phys. Lett. **B483** (2000) 124-130, (hep-ph/0004047).  
A. van Hameren and R. Kleiss, *Generating QCD-antennas*, Eur. Phys. J. **C17** (2000) 611-621, (hep-ph/0008068).

- [7] W.J. Stirling, R. Kleiss and S.D. Ellis, *A new Monte Carlo treatment of multiparticle phase space at high energy*, Comp. Phys. Comm. **40** (1986) 359.
- [8] H. Kharraziha and S. Moretti, *The metropolis algorithm for on shell momentum phases space*, Comp. Phys. Comm. **127** (2000) 242-260
- [9] L. Devroye, *Non-Uniform Random Variate Generation*, (Springer, 1986).

## 6 Appendices

### A Multi-channeling for importance sampling

In [1], the multi-channel method was constructed such that the variance of the Monte Carlo estimator of the integral of a function is minimal. We briefly repeat the line of argument. A sample of data points  $\boldsymbol{\omega} = (\omega_1, \omega_2, \dots, \omega_N)$  is generated distributed following the density  $G_x$ , and the integral of integrand  $P$  over  $\Omega$  is estimated by

$$\langle P/G_x \rangle_{\boldsymbol{\omega}} := \frac{1}{N} \sum_{i=1}^N \frac{P(\omega_i)}{G_x(\omega_i)} \xrightarrow{N \rightarrow \infty} \int_{\Omega} P(\omega) d\omega .$$

The variance of the estimator is given by

$$\frac{1}{N} \left( \int_{\Omega} \frac{P(\omega)^2}{G_x(\omega)} d\omega - \left( \int_{\Omega} P(\omega) d\omega \right)^2 \right) , \quad (8)$$

and extremization leads to the solution that the quantities

$$W_i(P, G_x) := \int_{\Omega} \frac{g_i(\omega) P(\omega)^2}{G_x(\omega)^2} d\omega$$

have to be equal for all  $i = 1, \dots, n$ . If  $G_x$  is a histogram, then the solution is immediately found using Algorithm 1 with the first step replaced by

**Algorithm 3 (importance sampling by variance optimization)**

1.  $y_i \leftarrow x_i \sqrt{W_i(P, G_x)}$  for all  $i = 1, \dots, n$

which is also applied in the general case. Of course the  $W_i(P, G_x)$  cannot be calculated exactly, but can be estimated by  $\langle g_i P^2 / G_x^3 \rangle_{\boldsymbol{\omega}}$ , since  $\boldsymbol{\omega}$  is distributed following  $G_x$ .

## B HICOM

In the Hierarchical Construction Of Momenta, one uses the fact that the phase space can be decomposed as

$$\begin{aligned}
d\Phi_n(P; \sigma_1, \dots, \sigma_n; p_1, \dots, p_n) &= ds_{n-1} d\Phi_2(P; \sigma_n, s_{n-1}; p_n, Q_{n-1}) \\
&\times ds_{n-2} d\Phi_2(Q_{n-1}; \sigma_{n-1}, s_{n-2}; p_{n-1}, Q_{n-2}) \\
&\vdots \\
&\times ds_2 d\Phi_2(Q_3; \sigma_3, s_2; p_3, Q_2) d\Phi_2(Q_2; \sigma_2, \sigma_1; p_2, p_1) ,
\end{aligned} \tag{9}$$

where

$$d\Phi_2(Q; s_1, s_2; q_1, q_2) := d^4q_1 \delta(q_1^2 - s_1) \theta(q_1^0) d^4q_2 \delta(q_2^2 - s_2) \theta(q_2^0) \delta^4(Q - q_1 - q_2)$$

is the standard two-body phase space. This decomposition tells us that if the variables involved are generated in this order and with these dependencies, then the final momenta are distributed on the desired bounded  $(3n - 4)$ -dimensional subspace of  $\mathbf{R}^{4n}$ . It does not tell us how the momenta are distributed, and there is the freedom how to generate the variables in each of the two-body phase spaces, and the variables  $s_i$ . Examples of particular choices to obtain momenta that are distributed following the antenna pole structure can be found in [2].

A well-known example how to generate each of the two-body phase spaces is by generating an angle  $\varphi$  uniformly in  $[0, 2\pi]$ , and a variable  $z$  distributed uniformly in  $[-1, 1]$ , performing the construction

$$\begin{aligned}
|\vec{q}_1| &\leftarrow \sqrt{\lambda(Q^2, s_1, s_2)/4/Q^2} \\
q_1^0 &\leftarrow \sqrt{s_1 + |\vec{q}_1|^2} \\
\vec{q}_1 &\leftarrow |\vec{q}_1| \left( \sqrt{1 - z^2} \cos \varphi, \sqrt{1 - z^2} \sin \varphi, z \right) ,
\end{aligned}$$

boosting  $q_1$  to the center-of-mass frame of  $Q$ , and putting  $q_2 = Q - q_1$ . The symbol  $\lambda$  stands for the standard Källén function. This construction gives a Jacobian factor  $2Q^2/\pi/\sqrt{\lambda(Q^2, s_1, s_2)}$  in the density. If we look at the decomposition (9) in the case that all squared masses  $\sigma_i$  are zero, we see that the Jacobian factors are equal to  $2Q_i^2/\pi/(Q_i^2 - s_{i-1})$ . Since  $Q_i^2 = s_i$  in the end, we see that the non-constant parts of the Jacobian factors cancel if the variables  $s_i$  are generated following the density

$$i(i-1) \frac{(s_{i+1} - s_i)(s_i)^{i-2}}{(s_{i+1})^i} ,$$

leading to momenta that are uniformly distributed over phase space with constant density

$$\frac{(n-1)(n-2)2P^2}{(P^2)^{n-1}\pi} \cdot \frac{(n-2)(n-3)2}{\pi} \dots \frac{(2)(1)2}{\pi} \cdot \frac{2}{\pi} = \left(\frac{2}{\pi}\right)^{n-1} \frac{\Gamma(n)\Gamma(n-1)}{(P^2)^{n-2}} .$$

The density for the variable  $s_i$  is obtained by generating  $\rho \in [0, 1]$  following the *beta*-density  $\beta_{i-1,2}(\rho) = i(i-1)(1-\rho)\rho^{i-2}$ , and putting  $s_i \leftarrow s_{i+1}\rho$ .

Cheng's BA algorithm [9] is very efficient in generating random numbers following *beta*-distributions. However, it uses the method of rejection and needs, on the average, more than one uniformly distributed random number for returning one *beta*-variable. What we would like is a direct construction with one random number as input, and the *beta*-variable as output, so that we can let PARNI deliver the input. Fortunately, Cheng's BA algorithm is so efficient that we can skip the rejection part, and just use its construction of a variable that is almost a *beta*-variable. If necessary, PARNI will compensate for that. For a general *beta*-density

$$\beta_{a,b}(\rho) \propto (1 - \rho)^{b-1} \rho^{a-1} ,$$

The density for the almost-*beta*-variable is given by

$$\frac{d}{d\rho} \frac{\rho^u}{\rho^u + (a/b)^u (1 - \rho)^u} ,$$

with

$$u = \begin{cases} \min(a, b) & \text{if } \min(a, b) \leq 1 \\ \sqrt{(2ab - a - b)/(a + b - 2)} & \text{if } \min(a, b) > 1 \end{cases} .$$